Reconstructing palaeochannel morphology with a mobile multicoil electromagnetic induction sensor

Philippe De Smedt [a,*], Marc Van Meirvenne [a], Eef Meerschman [a], Timothy Saey [a], Machteld Bats [b], Mona Court-Picon [c], Jeroen De Reu [b], Ann Zwertvaegher [c], Marc Antrop [d], Jean Bourgeois [b], Philippe De Maeyer [d], Peter A. Finke [c], Jacques Verniers [c], Philippe Crombé [b]

[a] Research Group Soil Spatial Inventory Techniques, Department of Soil Management, Ghent University, Coupure 653, 9000 Ghent, Belgium
[b] Department of Archaeology, Ghent University, Sint-Pietersnieuwstraat 35, 9000 Ghent, Belgium
[c] Department of Geology and Soil Science, Ghent University, Krijgslaan 281, 9000 Ghent, Belgium
[d] Department of Geography, Ghent University, Krijgslaan 281, 9000 Ghent, Belgium

ARTICLE INFO

ABSTRACT

Field methods to map and reconstruct the morphology of buried river systems are highly dependent on spatial interpolation. Conventional methods, such as standard borehole survey, allow a detailed vertical reconstruction of the shallow subsurface but leave lateral connections between sample locations open to interpretation. Geophysical survey techniques have recently introduced more detail. Mobile electromagnetic induction (EMI) survey combines high density sampling with full lateral coverage but fails to produce detailed information about vertical facies changes. Recently, multicoil EMI survey added vertical discrimination potential to this lateral continuity. In this study, we present an integrated approach for reconstructing the morphology of a known palaeochannel segment by modelling the depth to the sandy substrate. In addition, a calibration method based on a limited number of auger data is proposed. In a first phase, the modelling procedure was evaluated along two transects on a test site, showing palaeochannel depths ranging from 1 to >4 m beneath the surface. In a second phase, the morphology of the entire site was reconstructed. These three resulting depth models were then compared with auger observations and electrical resistivity tomography (ERT) data. The high correlation coefficients (>0.9) between observed and modelled depths showed that even in complex pedological environments, palaeochannel morphology could be predicted precisely using multicoil EMI data. Therefore, we concluded that a multicoil EMI survey proves to be an efficient and reliable solution for mapping and reconstructing the morphology of the shallow subsurface.

© 2011 Elsevier B.V. All rights reserved.

1. Introduction

Mapping the lithology and morphology of Quaternary deposits continues to challenge researchers studying the geomorphological and environmental characteristics of the palaeolandscape. Conventional techniques to map these deposits include methods such as augering or coring (Berendsen and Stouthamer, 2001) and more recently developed surveys based on near-surface geophysics (e.g., Gourry et al., 2003; Howard et al., 2008).

Augering allows a detailed and accurate registration of vertical lithological variation. However, low sampling density from the time-consuming character of this method, leaves the interpretation of lateral variations dependent on interpolation methods used for producing maps (Baines et al., 2002). These limitations also apply to electrical resistivity tomography (ERT). Although this technique incorporates more of the lateral variation present, a high measurement density across the entire survey area is rare.

Non-invasive methods such as ground penetrating radar (GPR) and methods based on electromagnetic induction (EMI) do enable a more continuous mapping of the lithological variation by generating a higher sampling density in a mobile configuration, but, these also have some limitations (Schrott and Sass, 2008). Clay layers and a high level of water saturation can lead to a stronger attenuation of GPR signals, which especially restricts the application of this technique on alluvial deposits (Moorman, 1990; Howard et al., 2008; Schrott and Sass, 2008). On the other hand, EMI prospection is not hampered by water and clay content but sometimes does not produce sufficient information about vertical facies changes (Conyers et al., 2008). This lack of vertical discrimination potential particularly applies to EMI systems such as the EM31 (Geonics, Toronto, Canada) that only have one single coil pair (transmitter–receiver) determining the depth of exploration (McNeill, 1980). When a frequency-domain EMI system with a multicoil configuration is integrated into a mobile field setup, two major mapping limitations can be avoided. Lateral soil variability

* Corresponding author. Tel.: +32 92646042; fax: +32 92646247.
E-mail address: Philippe.DeSmedt@UGent.be (P. De Smedt).

can be continuously mapped at a high resolution by measuring changes in soil apparent electrical conductivity (σ_a), thus eliminating the possible interpolation error caused by a low sampling density (Simpson et al., 2008; Saey et al., 2009). Furthermore, the integration of multiple coil pairs with different vertical sensitivities generates conductivity measurements of different sediment volumes. If the measurements resulting from each coil pair are then compared, soil conductivity can be accurately modelled at different depths (Saey et al., 2009).

The current study is part of a project that aims to construct the geomorphological, pedological, and environmental evolution of Late Glacial palaeomire against the background of its archaeological importance throughout prehistory (more detailed information about the project can be found in Bats et al., 2009). An important part of this research project is the detection and geomorphological investigation of palaeoriver systems. The general aim of the geophysical fieldwork is to map these river systems and describe their morphology, enabling an evaluation of their impact on the former landscape.

In this study the focus lies on the vertical sensitivity of the applied geophysical technique. Multicoil EMI data will be used to model the depth of a palaeoriver segment. More specifically, a two-layer model will be composed to reconstruct the depth to the sandy substrate through which the palaeoriver segment has been cut out. In addition, a calibration method based on auger data will be introduced to adjust the modelling parameters and increase the model's accuracy. This study constitutes a novel contribution to mapping near surface deposits by adding a vertical dimension to a continuous EMI based mapping technique.

2. Study area

The palaeomire (Moervaart, Belgium) (Fig. 1) is characterised by a diverse pedology and geomorphology (Heyse, 1983). The area consists of Quaternary coversands and paleomire sediments containing up to 45% $CaCO_3$. In these Quaternary palaeomire deposits, traces of several palaeorivers can be found that are related to the Late Glacial and the early Holocene. These traces are mostly located just beneath the plough layer, and sometimes peaty outcrops related to the buried channels can still be seen in the landscape. As with the palaeomire itself, the morphology of these palaeorivers and the sedimentological composition of their infillings show a large variability. With palaeo-channel depths ranging from around 1 to >7 m and river types varying from braided systems to straight and alluvial streams, the area is a testimony of a complex hydrological evolution. The pedological variation of the infillings, often made up of different peat and gyttja layers and laminated silt packages, adds up to the heterogeneity of the system.

Based on the digital elevation model (DEM) (Werbrouck et al., 2011), a test site of 0.45 ha was selected at the boundary of the palaeomire (Fig. 1). Here, DEM data suggested the presence of a branch of the palaeoriver system intersecting the field.

3. Methodology

Because of the complex sedimentology of the study area, two types of near-surface geophysical methods were selected: ERT and EMI; GPR was excluded because of the high clay percentages and the frequent water-saturated conditions (Moorman, 1990; Schrott and Sass, 2008). In addition to these methods, hand augering was performed for further interpretation of the geophysical data.

3.1. Multicoil electromagnetic induction survey

Because the applied methodology needs to combine a high lateral spatial resolution with accurate vertical measurements, a mobile multicoil EMI survey was employed as the main technique. We used a Dualem-21S EMI sensor (Dualem, Canada), which is a low induction number, frequency-domain EMI sensor. This sensor creates a primary electromagnetic field (H_p) in the transmitter coil, which induces a secondary electromagnetic field (H_s) in the soil. The magnitude of this secondary field is measured by the receiver coils and is assumed to be directly proportional to σ_a (McNeill, 1980).

The four receiver coils of the Dualem-21S are placed at distances of 1, 1.1, 2, and 2.1 m from the transmitter coil (Fig. 2). The receiver coils placed at 1 and 2 m distance, each form a coil pair in a horizontal coplanar (HCP) loop orientation with the transmitter coil (1 and 2 HCP respectively). The coils placed at 1.1 and 2.1 m from the transmitter coil, form pairs in a perpendicular (PERP) loop orientation (1.1 and 2.1 PERP) (Simpson et al., 2009). Because the intercoil separation and the orientation of the transmitter and the receiver coils, together with the height of the instrument above the ground, directly influence their spatial sensitivity (Gebbers et al., 2007; Monteiro Santos et al., 2010), the combination of multiple coil configurations allows measuring different soil volumes simultaneously.

The cumulative response of a layered medium up to a depth (z) below a certain coil pair can be determined by using the depth response functions defined by McNeill (1980). These response functions have been proven valid in both homogeneous and heterogeneous soil (Hendrickx et al., 2002) and are assumed to be independent of soil electrical conductivity when operating at low induction numbers (McNeill, 1980; Callegary et al., 2007). The actual depth of exploration (DOE) for a certain coil pair is arbitrarily defined as the depth at which 70% of the total signal response is obtained from the soil volume above this depth (Saey et al., 2009). For the Dualem sensor, the DOE varies from 0.54 to 1.03 m for the PERP coil configurations and from 1.55 to 3.18 m for the HCP modes, allowing detection of vertical σ_a variations by integrating the multiple signals.
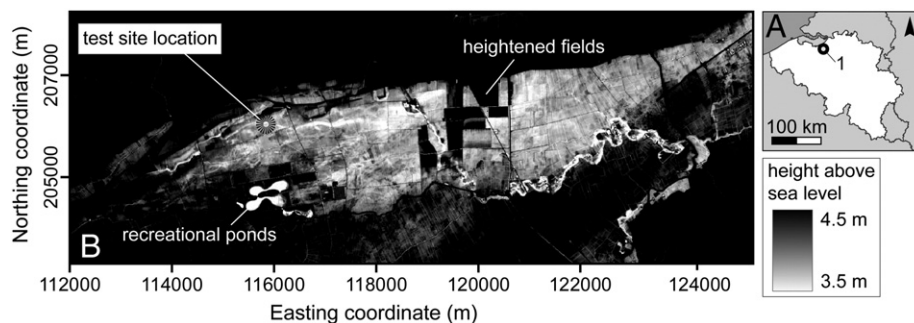

Fig. 1. (A) Localisation of the test site in Belgium. (B) DEM of the Moervaart palaeomire, visible as the east–west oriented depression, with localisation of the test site (coordinates are according to the Belgian metric Lambert 72 projection).
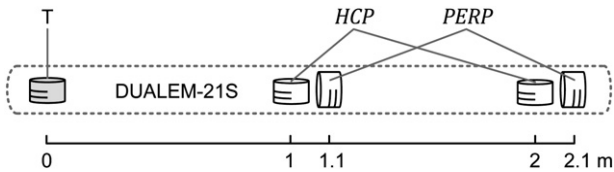
Fig. 2. Schematic representation of the Dualem-21S sensor with the transmitter coil (T) and the four receiver coils (in *HCP* and *PERP* loop orientation with T).

To combine this vertical discrimination potential with a high spatial resolution, field measurements were conducted with a mobile setup that enabled recording four bulk conductivity values every 0.20 m, i.e., one measurement with each coil pair every second. By driving over the test site in parallel lines with a 2-m separation, a nearly complete lateral coverage of the site was achieved. In this configuration and at this resolution it was possible to map 1 ha every hour. Field data were then processed and combined in four σ_a maps (Fig. 3). Based on these maps, two 65-m sections were set up (Section 1, S1, and Section 2, S2), along which palaeochannel depth would be modelled (Fig. 3A). Section 1 was set up over the palaeoriver segment's maximum extent as represented in the σ_a maps, whereas in S2 a smaller part of the feature would be investigated.

3.2. Hand augering and electrical resistivity tomography

Auger locations along both sections that covered the range of σ_a values were selected for model calibration and evaluation. On each transect, seven calibration and eight evaluation hand augerings were drilled with a 2-cm gouge auger (Fig. 3A).

For further evaluation, ERT (Baines et al., 2002; Samouëlian et al., 2005) was performed on both sections. These data were used to detect inconsistencies between the modelled depths and the ERT pseudosection at locations where no auger data were available. We used a Terrameter SAS 1000 LUND imaging system (ABEM instruments AB, Sundbyberg, Sweden). Each ERT transect consisted of 64 electrodes that were connected to a resistivity meter by an electrode selector system, enabling the automatic measurement of the soil apparent resistivity in a Wenner–Schlumberger configuration (Samouëlian et al., 2005).

As the ERT was carried out across a known palaeochannel segment, the electrode spacing was defined based on the auger data to match both the width and the depth of the feature. This resulted in two 63-m ERT sections with a 1-m electrode spacing (Fig. 3A). The inversion of the apparent resistivity data to modelled vertical sections was done with RES2DINV software (Geotomo software, Malaysia), following the method of Loke and Barker (1996).

3.3. Modelling the depth of a predefined soil layer

To model the morphology of the palaeochannel, we assumed a two-layered soil system. The palaeochannel infillings and the loamy sediments overlaying most of the site were considered as the top layer (i_{top}), while the substrate (i_{sub}) was defined as the Quaternary sand through which the palaeorivers were incised. The objective was to model the depth to i_{sub}, i.e., z_{sub}. Therefore, the contribution of each layer's conductivity to σ_a was considered. Given the conductivity of the top layer (σ_{top}) and the substrate (σ_{sub}), this relationship can be defined by the cumulative response (R) up to z_{sub} for any coil configuration (x) with intercoil separation (s) (McNeill, 1980; Saey et al., 2008):

$$R_{x,s}(z_{sub}) = \frac{\sigma_a - \sigma_{top}}{\sigma_{sub} - \sigma_{top}} \qquad (1)$$

Saey et al. (2008) combined these response functions (Eq. (1)), taking the sensor height above the surface (z_α) into account, to

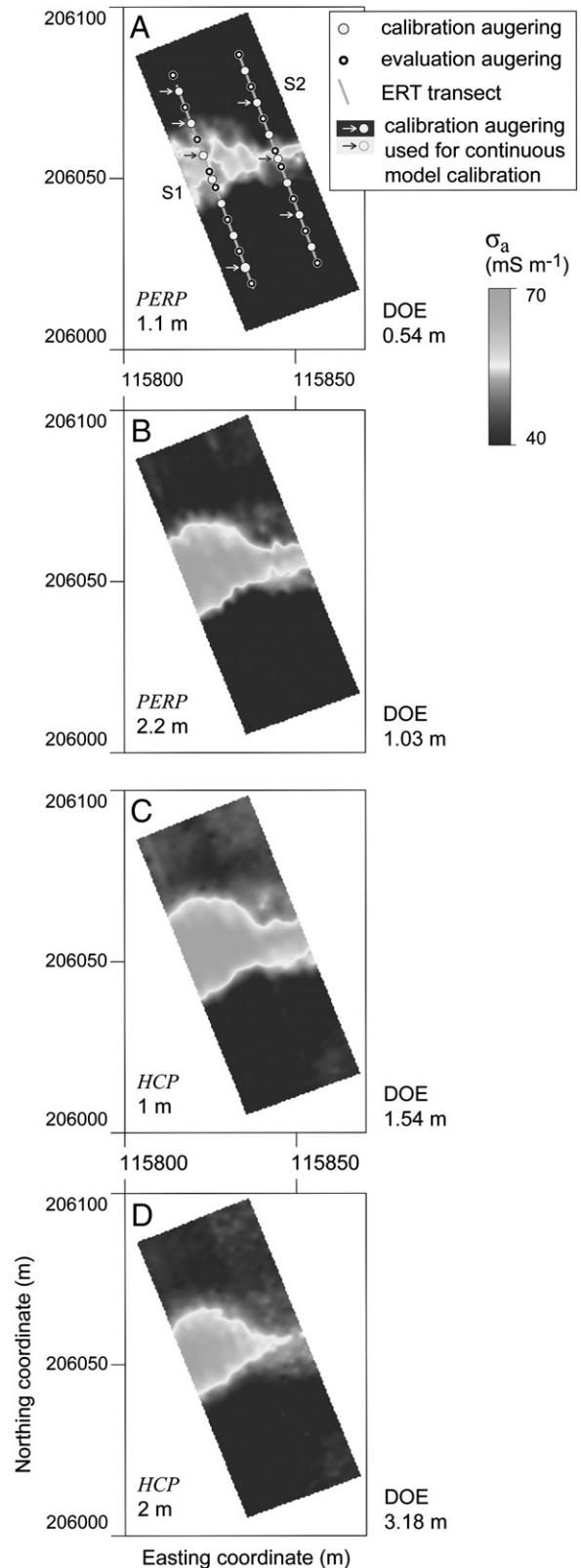**Fig. 3.** σ_a maps of each of the four coil configurations of the Dualem-21S EMI sensor. Fig. 3A also shows the auger locations and the ERT transects.

predict the depth of a predefined soil layer. For *HCP* configurations, this predicted depth (z_{sub}^*) can be found with

$$z_{sub}^* = s\left[\frac{1}{4R_{HCP}(z_{sub}^*)^2} - \frac{1}{4}\right]^{0.5} - z_\alpha \qquad (2)$$

and for *PERP* coil configurations with

$$z_{sub}^* = s \left[\frac{R_{PERP,s}}{\left(2\left(1 - R_{PERP}\left(z_{sub}^*\right)^2\right)\right)^{0.5}} \right] - z_\alpha \qquad (3)$$

To obtain z_{sub}^*, both σ_{top} and σ_{sub} had to be estimated and entered into the modelling equation. A common method to determine these conductivities is EC-probing, but this was impossible because of the high and strongly fluctuating groundwater level at the test site. Therefore, theoretical top layer (σ_{top}^t) and substrate (σ_{sub}^t) conductivity values were modelled by minimising the difference between the observed z_{sub} and the modelled z_{sub}^* for each coil configuration separately (Saey et al., 2008).

For each section, the seven calibration observations (z_{sub}) were plotted as a function of the measured σ_a at these locations per coil configuration. Next, theoretical response curves were fitted to the calibration data by iteratively adjusting bulk conductivity values (σ_a^t) under the predefined assumptions that σ_{top} is higher than σ_{sub} and that both layers' conductivity values are homogeneous throughout each section.

These theoretical σ_a were then used to determine z_{sub}^* along both sections. At each measurement location, the four Dualem conductivity values were combined and entered into Eq. (4) per coil pair (x,s) in order to model z_{sub}^*:

$$\sigma_a = \left[R_{x,s}(z_a) - R_{x,s}(z_{sub}^* + z_a) \right] \cdot \sigma_{top}^t + \left[R_{x,s}(z_{sub}^* + z_a) \right] \cdot \sigma_{sub}^t \qquad (4)$$

The resulting depth models were then evaluated with auger data from eight locations for each section to determine the correlation coefficient and the root mean square estimation error (RMSEE) between the modelled and observed substrate depths.

After applying this methodology to both sections, a depth model was composed for the entire test site. Again calibration data from seven locations (Fig. 3A) were used to determine σ_{top} and σ_{sub} of the entire site with the same calibration procedure as applied on S1 and S2. The remaining auger data (23 locations) were used for model evaluation.

4. Results and discussion

The EMI survey revealed the presence of a palaeochannel on all four σ_a maps (Fig. 3A–D). In addition, two lithological profiles were composed based on the auger data (Fig. 4). The laminated deposits of the palaeoriver were made up of silty to loamy sediments overlain with surfacing peat. In S1, these fine-grained infillings were found over a width of 32 m, with a maximum depth to the sandy substrate of 4.6 m. In S2, the palaeochannel's infillings extended over 20 m of the section and were observed to a maximum depth of 1.27 m. Within the channel deposits, marly and organic layers as well as clay bands could be observed. At both sides of the palaeochannel, the slightly silty sand layers that separate the substrate from the loamy plough layer were interpreted as levee deposits. At these locations, the depth of i_{sub} was based on the depth of the levee deposits because of the textural similarities between these deposits and the substrate. In both sections, the transition zone between i_{top} and i_{sub} was marked by a gradual textural change with sand content increasing with depth.

For each section, the seven calibration z_{sub} values were fitted to response curves (Eq. (1)) per coil configuration using the modelled σ_{top}^t and σ_{sub}^t (Fig. 5). The resulting depth models were then evaluated with auger data and compared to the ERT pseudosections (Fig. 6).

In S1 (Fig. 6 top), model evaluation resulted in a correlation coefficient between z_{sub} and z_{sub}^* of 0.96 and an RMSEE of 0.56 m. For S2 (Fig. 6 bottom), a correlation coefficient of 0.97 and an RMSEE of 0.11 m were found. Although the ERT pseudosection for S2 slightly overestimated the palaeochannel depth, ERT data confirmed the modelled morphology for both sections (Fig. 6). However, in S1 the influence of the limited DOE of the sensor could be seen. Compared to the ERT data, this model showed a local deviation around 45–55 m along the transect. In general, local model precision for S1 lessened at increasing depths, but the overall morphology of the palaeochannel was well represented. In S2, depths never surpassed 2 m, which enabled a more precise modelling over the entire depth range. This limitation can be avoided by using multicoil EMI sensors with a larger DOE (e.g., Monteiro Santos et al., 2010) but at the cost of a lower measurement resolution.

Next we modelled z_{sub}^* for the entire test site. Based on seven calibration values, σ_{top}^t and σ_{sub}^t were determined. The resulting depth model (Fig. 7) was evaluated at the remaining 23 auger locations
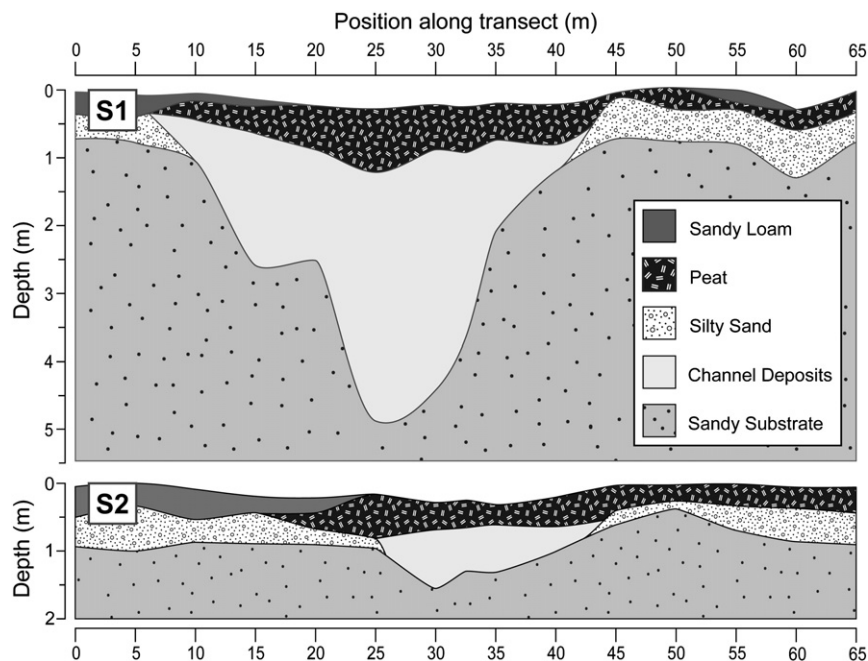

Fig. 4. Schematic lithological profile of the palaeochannel in S1 (top) and S2 (bottom) based on auger data.
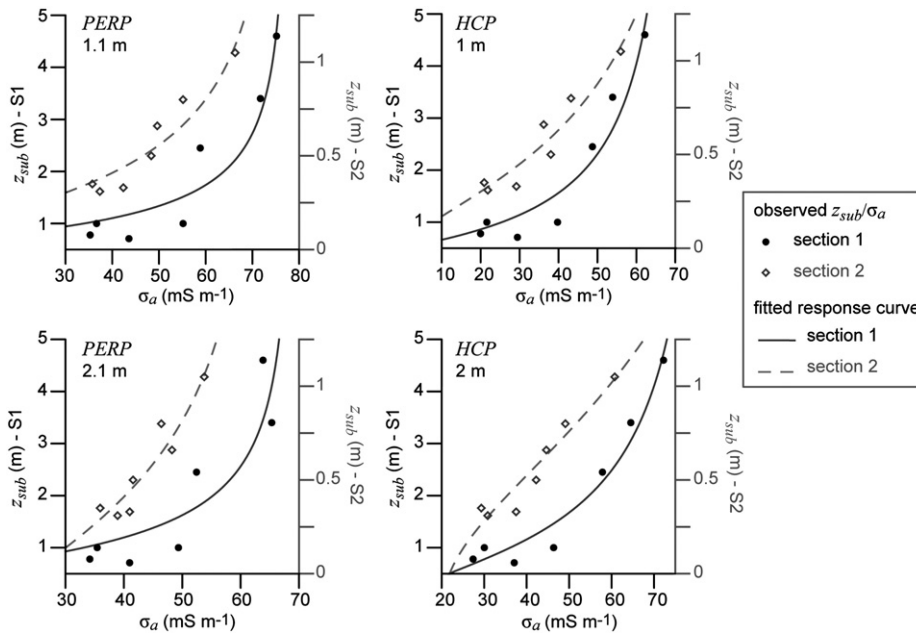
Fig. 5. Observed depths to i_{sub} with observed σ_a at the auger calibration locations with fitted response curves for both sections.
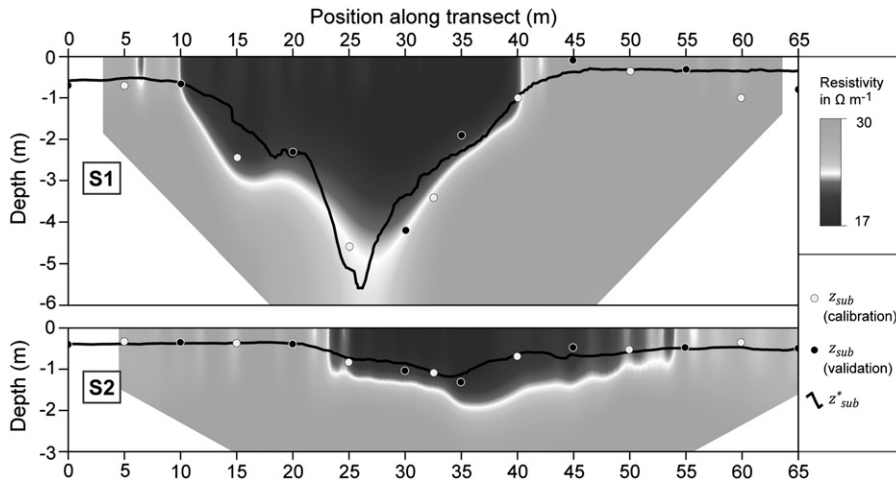

Fig. 6. ERT resistivity profile with observed and modelled palaeochannel depths for S1 (top) and S2 (bottom).

(Fig. 3A). Fig. 8 shows the correlation between the modelled and the observed depths at these locations. Whereas at small depths z_{sub} was often overestimated in the continuous model, greater depths to the substrate tended to be underestimated, indicating a general smoothing effect of the modelled morphology. Still, a correlation coefficient of 0.93 and an RMSEE of 0.41 m between the modelled depths and the evaluation data confirmed the precision of the model in predicting the soil morphology. The model clearly showed the morphology of the
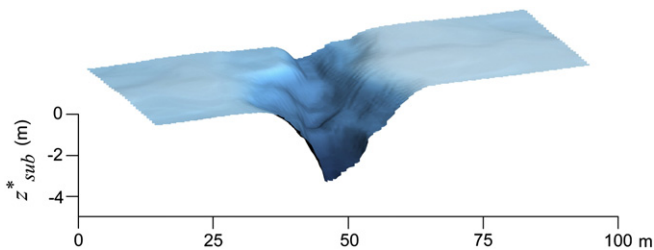

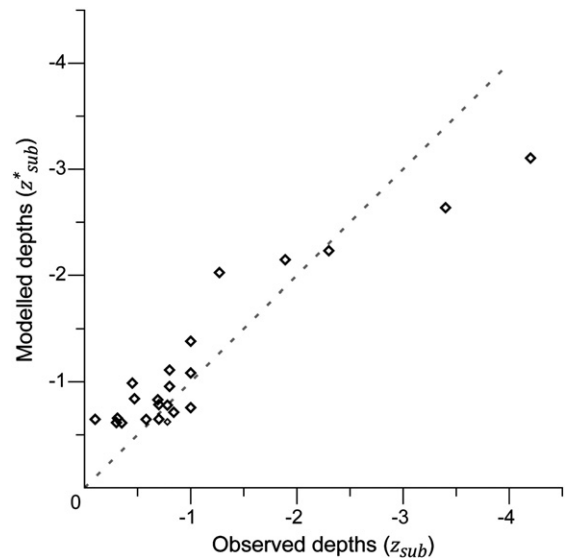**Fig. 7.** Continuous depth model of the test site.

Fig. 8. Scatter plot of the observed and modelled depths for the continuous model.

site and the width and gradient of the palaeochannel. Even with the sensor's limited DOE, the method allowed us to accurately model the depth to predefined soil layers.

5. Conclusions

The predicted depth to the substrate along both modelled sections, as well as the continuous model, showed a strong correlation to the evaluation data. Especially by introducing auger data as a calibration method in the modelling process, local precision was added and the accuracy of predicting palaeochannel depths could be extended beyond the instrument's DOE. Combined with the spatial resolution of a mobile survey, multicoil EMI allows high resolution exploration of the shallow subsurface, which is demonstrated by the continuous depth model. However, the general smoothing effect observed in this model hints at the limitations of the method in predicting soil layer depths in complex pedological environments and with depths exceeding the DOE. Despite this drawback, the overall model precision was very good, providing unique insights into the test site's morphology. The presented results show that the mobile multicoil EMI survey combined with the proposed modelling sequence can be an efficient tool to map buried sediments and land surfaces. In particular, buried fluvial systems can this way be extensively and accurately traced throughout the landscape.

Acknowledgements

References

Baines, D., Smith, D.G., Froese, D.G., Bauman, P., Nimeck, G., 2002. Electrical resistivity ground imaging (ERGI): a new tool for mapping the lithology and geometry of channel-belts and valley-fills. Sedimentology 49, 441–449.

Bats, M., De Reu, J., De Smedt, P., Antrop, M., Bourgeois, J., Court-Picon, M., De Maeyer, P., Finke, P., Van Meirvenne, M., Verniers, J., Werbrouck, I., Zwertvaeger, A., Crombé, P., 2009. Geoarchaeological research of the large palaeolake of the Moervaart (municipalities of Wachtebeke and Moerbeke-Waas, East-Flanders, Belgium). From Late Glacial to Early Holocene. Notae Praehistoricae 29, 105–112.

Berendsen, H.J.A., Stouthamer, E., 2001. Palaeogeographic Development of the Rhine-Meuse Delta, the Netherlands. Van Gorcum, Assen, The Netherlands.

Callegary, J.B., Ferre, T.P.A., Groom, R.W., 2007. Vertical spatial sensitivity and exploration depth of low-induction-number electromagnetic-induction instruments. Vadose Zone Journal 6, 158–167.

Conyers, L.B., Ernenwein, E.G., Grealy, M., Lowe, K.M., 2008. Electromagnetic conductivity mapping for site prediction in meandering river floodplains. Archaeological Prospection 15, 81–91.

Gebbers, R., Lück, E., Heil, K., 2007. Depth sounding with the EM38-detection of soil layering by inversion of apparent electrical conductivity measurements. In: Stafford, J.F. (Ed.), Precision Agriculture '07. Wageningen Academic Publishers, Wageningen, The Netherlands, pp. 95–102.

Gourry, J.-C., Vermeersch, F., Garcin, M., Giot, D., 2003. Contribution of geophysics to the study of alluvial deposits: a case study in the Val d'Avaray area of the River Loire, France. Journal of Applied Geophysics 54, 35–49.

Hendrickx, J.M.H., Borchers, B., Corwin, D.L., Lesch, S.M., Hilgendorf, A.C., Schlue, J., 2002. Inversion of soil conductivity profiles from electromagnetic induction measurements: theory and experimental verification. Soil Science Society of America Journal 66, 673–685.

Heyse, I., 1983. Preliminary results of the study of a Vistulian Late Glacial drainage pattern in the Scheldtbasin (Belgium - Flemish Valley - Moervaart Depression). Quaternary Studies in Poland 4, 135–143.

Howard, A.J., Brown, A.G., Carey, C.J., Challis, K., Cooper, L.P., Kincey, M., Toms, P., 2008. Archaeological resource modelling in temperate river valleys: a case study from the Trent valley (UK). Antiquity 318, 1040–1054.

Loke, M.H., Barker, R.D., 1996. Rapid least-squares inversion of apparent resistivity pseudosections by a quasi-Newton method. Geophysical Prospecting 44, 131–152.

McNeill, J.D., 1980. Electromagnetic terrain conductivity measurement at low induction numbers. Technical Note 6, Geonics Limited, City, Ontario, Canada.

Monteiro Santos, F.A., Triantafilis, J., Bruzgulis, K.E., Roe, J.A.E., 2010. Inversion of multiconfiguration electromagnetic (DUALEM-421) profiling data using a one-dimensional laterally constrained algorithm. Vadose Zone Journal 9, 117–125.

Moorman, B.J., 1990. Assessing the ability of ground penetrating radar to delineate subsurface fluvial lithofacies. M.Sc. Thesis, The University of Calgary, Calgary, AB, Canada, 124 pp.

Saey, T., Simpson, D., Vitharana, U.W.A., Vermeersch, H., Vermang, J., Van Meirvenne, M., 2008. Reconstrucing the palaeotopography beneath the loess cover with the aid of an electromagnetic induction sensor. Catena 74, 58–64.

Saey, T., Simpson, D., Vermeersch, H., Cockx, L., Van Meirvenne, M., 2009. Comparing the EM38DD and Dualem-21 S sensors for depth-to-clay mapping. Soil Science Society of America Journal 73, 7–12.

Samouëlian, A., Cousin, I., Tabbagh, A., Bruand, A., Richard, G., 2005. Electrical resistivity survey in soil science: a review. Soil and Tillage Research 83, 173–193.

Schrott, L., Sass, O., 2008. Application of field geophysics in geomorphology: advances and limitations exemplified by case studies. Geomorphology 93, 55–73.

Simpson, D., Lehouck, A., Van Meirvenne, M., Bourgeois, J., Thoen, E., Vervloet, J., 2008. Geoarchaeological prospection of a medieval manor in the Dutch Polders using an electromagnetic induction sensor in combination with soil augerings. Geoarchaeology 23, 1–14.

Simpson, D., Van Meirvenne, M., Saey, T., Vermeersch, H., Bourgeois, J., Lehouck, A., Cockx, L., Vitharana, U.W.A., 2009. Evaluating the multiple coil configurations of the EM38DD and DUALEM-21 S sensors to detect archaeological anomalies. Archaeological Prospection 16, 91–102.

Werbrouck, I., Antrop, M., Van Eetvelde, V., Stal, C., De Maeyer, P., Bats, M., Bourgeois, J., Court-Picon, M., Crombé, P., De Reu, J., De Smedt, P., Finke, P.A., Van Meirvenne, M., Verniers, J., Zwertvaegher, A., 2011. Digital elevation model generation for historical landscape analysis based on LiDAR data, a case study in Flanders (Belgium). Expert Systems with Applications 38, 8178–8185.